ChemComm

ROYAL SOCIETY OF CHEMISTRY

FEATURE ARTICLE

View Article Online
View Journal | View Issue

Published on 23 December 2021. Downloaded by Technical University of Munich on 2/3/2022 3:20:27 PM.

Check for updates

Cite this: *Chem. Commun.*, 2022, **58**, 1284

Carbodiimide-fueled catalytic reaction cycles to regulate supramolecular processes

Patrick S. Schwarz,[a] Marta Tena-Solsona,[a] Kun Dai[a] and Job Boekhoven *[ab]

Received 15th November 2021,
Accepted 15th December 2021

DOI: 10.1039/d1cc06428b

rsc.li/chemcomm

Using molecular self-assembly, supramolecular chemists can create Gigadalton-structures with angstrom precision held together by non-covalent interactions. However, despite relying on the same molecular toolbox for self-assembly, these synthetic structures lack the complexity and sophistication of biological assemblies. Those assemblies are non-equilibrium structures that rely on the constant consumption of energy transduced from the hydrolysis of chemical fuels like ATP and GTP, which endows them with dynamic properties, *e.g.*, temporal and spatial control and self-healing ability. Thus, to synthesize life-like materials, we have to find a reaction cycle that converts chemical energy to regulate self-assembly. We and others recently found that this can be done by a reaction cycle that hydrates carbodiimides. This feature article aims to provide an overview of how the energy transduced from carbodiimide hydration can alter the function of molecules and regulate molecular assemblies. The goal is to offer the reader design considerations for carbodiimide-driven reaction cycles to create a desired morphology or function of the assembly and ultimately to push chemically fueled self-assembly further towards the bottom-up synthesis of life.

1. Introduction

In the past decades, we have mastered the principles of structure formation through the self-assembly of molecules. Structure formation in biology, like the folding of proteins[1] and their subsequent assembly,[2] formation of lipid bilayers,[3] or packing of the genome,[4] rely on similar rules and principles as the self-assembly of non-biological molecules. If anything, by using non-natural molecules, the diversity of building blocks is much greater. Why then are biological assemblies so much more sophisticated compared to man-made structures?

First, biological structure formation occurs through self-assembly over many length scales, and we have not mastered this so-called hierarchical self-assembly at all. The folding of the three peptide strands of type 1 collagen into right-handed

[a] *Department of Chemistry, Technical University of Munich, Lichtenbergstraße 4, 85748 Garching, Germany. E-mail: job.boekhoven@tum.de*
[b] *Institute for Advanced Study, Technical University of Munich, Lichtenbergstraße 2a, 85748, Garching, Germany*

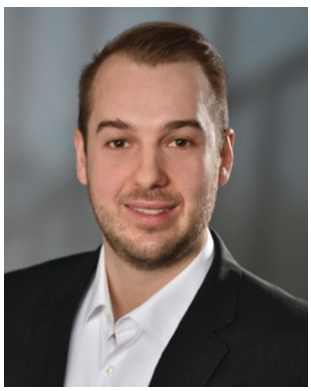

Patrick S. Schwarz

Patrick Schwarz graduated in Chemistry in 2015 at the Technical University of Munich. He obtained his master's degree under the guidance of Prof. Boekhoven in 2018 at the same university. After that, he continued his studies as a PhD student in Prof. Boekhoven's lab focusing on understanding and designing feedback mechanisms in chemically fueled self-assembly.



Marta Tena-Solsona

Dr Marta Tena-Solsona graduated in Chemistry in 2010 and obtained her master's degree in Pharmaceutical Chemistry in 2011 at Universitat Jaume I (Spain). In 2015, she got her PhD at the same university supervised by Prof. Beatriu Escuder and Juan Felipe Miravet. In 2016, she joined Prof. Boekhoven's Lab at the Technical University of Munich where she is currently working. Her main interests focus on the development of synthetic dissipative systems driven far from equilibrium by chemical reaction networks.

This journal is © The Royal Society of Chemistry 2022

Published on 23 December 2021. Downloaded by Technical University of Munich on 2/3/2022 3:20:27 PM.

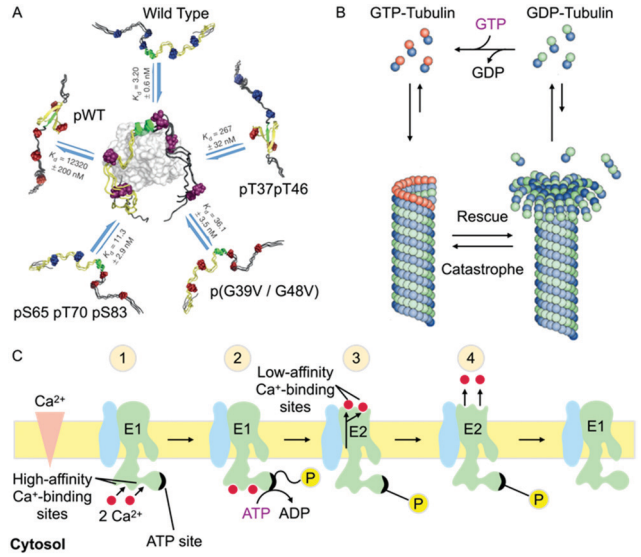

Fig. 1 Biological systems use energy from ATP and GTP hydrolysis to regulate folding, structure formation, and molecular machines. (A) Schematic representation of the folding of the 4E-BP2 protein (a major neural isoform of the family of three mammalian proteins) at different phosphorylation states and K_d values for the interaction with eIF4E (grey surface). Figure adapted from ref. 8 by permission of the Nature Publishing Group, Copyright © 2014. (B) Schematic representation of the GTP-driven structure formation of microtubules. Figure adapted from ref. 7*a* by permission from The Royal Society of Chemistry, Copyright © 2017. (C) Schematic representation of the ATP-driven operation of Ca^{2+} ATPase pumps as an example for a molecular machine. Figure adapted from ref. 9 by permission from W.H. Freeman and Company, Copyright © 2000.

α-helices, their subsequent trimerization by winding around one another in a collagen triple helix, and assembly of triple helices into collagen fibrils is an excellent example of mesoscopic biological structure formation.[5] We refer the reader to excellent reviews of synthetic hierarchical assemblies.[6] Secondly, biological structures are complicated mixtures of hundreds of components that each perform an indispensable role yet do not interfere with one another. This multicomponent self-assembly is another challenge that we have to master.

Finally, and the focus of this review, biological structures are not static in-equilibrium structures but endowed with dynamic functions, such as the ability to control structures temporally and spatially, to perform of work, to move, to self-heal, and to adapt.[7] These dynamic functions do not occur in equilibrium and thus require the transduction of energy.[7] Therefore, in recent years, methods by which energy can regulate molecular assemblies have been introduced in supramolecular chemistry.

1.1. Energy from a fuel-driven chemical reaction

Biology transduces energy to regulate molecular self-assembly. This energy typically originates from converting molecules with high chemical potential into molecules with lower chemical potential. We will refer to these high-energy molecules as "fuels." The canonical biological fuels are ATP and GTP, whose energy is liberated through hydrolysis into ADP, GDP, and inorganic phosphate. The stability of ATP prevents the spontaneous liberation of its energy. Instead, it is hydrolyzed through a catalytic cycle which is at the heart of the energy-transducing mechanism. For example, kinases can catalyze the hydrolysis of ATP to ADP, resulting in phosphorylation of a target which is used by biological systems as a post-translational modification to regulate the folding of proteins (Fig. 1A).[8] Moreover, biological systems use the transduced energy from ATP and GTP hydrolysis to regulate structure formation, *e.g.*, the dynamic instability of microtubules (Fig. 1B).[7a] Another example of such catalytic cycles in biology are molecular machines, *e.g.*, Ca^{2+} ATPase pumps. An ATPase can catalyze ATP hydrolysis in two steps, *i.e.*, in a first step, a nucleophile in the active center of the ATPase is phosphorylated, and in a second step, the phosphorylated nucleophile is hydrolyzed, liberating inorganic phosphate and the original enzyme (Fig. 1C).[9]



Kun Dai

Kun Dai graduated in chemical engineering in 2010 and obtained his master's degree in 2017 at Shaanxi Normal University (China). After that, he joined Prof. Boekhoven's Lab at the Technical University of Munich as a PhD student. He mainly focuses on the development of design rules in chemically fueled self-assembly.



Job Boekhoven

Prof. Dr Job Boekhoven is developing tools to regulate the self-assembly of molecules the way biology does. He is best known for his work on chemically fueled reaction cycles that control the ability of molecules to assemble or phase separate. The resulting materials show exciting new properties, such as their intrinsic ability to self-heal or their controllable lifetime. Moreover, the chemically fueled assemblies manifest features we usually associate with living cells, like the ability to emerge, decay, or even self-divide. He holds a PhD degree (2012) from Delft University of Technology and is currently an assistant professor at the Technical University of Munich.

Published on 23 December 2021. Downloaded by Technical University of Munich on 2/3/2022 3:20:27 PM.

From the perspective of the fuel, it has now liberated its energy. From the perspective of the enzyme, it was transiently phosphorylated in the process. If the enzyme changed its function upon phosphorylation, we have transduced the chemical energy stored in ATP into a temporary change in function. In the case of the Ca^{2+} ATPase, ATP is converted in a cascade of chemical reactions and changes the conformation of the ATPase such that it binds a calcium ion on the cytosolic side of the membrane and transports it to the other side of the membrane. In other words, the ATP is hydrolyzed, and the energy liberated is used to pump calcium from one side to the other side of a membrane, thereby creating a transmembrane calcium gradient. Importantly, the enzyme in such a catalytic reaction cycle is not altered and can undergo thousands of cycles.

1.2. The simplest chemically fueled catalytic reaction cycle

Biology uses catalytic reaction cycles that convert ubiquitous fuels into waste and use the energy to change the function of the catalyst transiently. A goal of supramolecular chemistry should thus be to find mechanisms by which simple high-energy molecules can be converted into waste in a catalytic reaction cycle that changes the function of a supramolecular catalyst. A catalytic reaction cycle would have to follow these design criteria:

(1) The fuel has to be (relatively) stable in the absence of the energy transducing molecule. ATP does not spontaneously hydrolyze on timescales of hours. In the absence of ATPases, it has a half-life of roughly 175 h in water at pH 8 and 25 °C.[10] This kinetic stability yet high thermodynamic instability is likely the reason why biology uses ATP, *i.e.*, it contains a large amount of energy but does not spontaneously decompose. Thus, a synthetic analog should be relatively stable and not spontaneously decompose. On the other hand, if the fuel is too stable, highly specialized catalysts are required to liberate its energy, limiting the scope of the catalyst.

(2) The fuel conversion should be catalyzed in at least two steps: activation and deactivation. The conversion of fuel should be a catalytic process. That means that the catalyst, *e.g.*, ATPase, should be recovered to its original state after the reaction cycle has completed. The simplest way to do so is with two chemical reactions: activation of the catalyst and subsequent deactivation of the catalyst. In the activation step, the fuel reacts with the catalyst and activates it. The fuel can either bind it, or part of the fuel molecule is bound, *e.g.*, it binds ATP, or the phosphate group is transferred. The activated catalyst is deactivated in the next step, reverting the catalyst to its previous state and completing the reaction path (*e.g.*, releasing the bound phosphate). Based on these requirements, several successful synthetic fuel-driven reaction cycles have been reported, *e.g.*, relying on phosphorylation and dephosphorylation of the catalytic precursor,[11] reduction and oxidation of the catalytic precursor,[12] methylation and hydrolysis of the catalytic precursor,[13] olefin metathesis of the catalytic precursor,[14] and reactions based on imine formation,[15] transacylation[16] and others.[17] These examples demonstrate the versatility of chemically fueled catalytic reaction cycles.

1.3. The aim of this feature article

One catalytic reaction cycle that has received a great amount of attention and is used by several groups is based on the hydration of a carbodiimide into its corresponding urea catalyzed by a carboxylate-based precursor. Given its popularity, this feature article aims to provide an overview of how the energy liberated in this catalytic reaction cycle has been used to alter the function of supramolecular constructs.

The feature article is structured as follows: In Section 2, we provide an overview of the types of carbodiimide-driven reaction cycles and design considerations. In Section 3, we show how the energy derived from carbodiimide hydration can fold molecules. In the section after, we highlight examples in which carbodiimide hydration regulates structure formation and show that self-assembled structures can exert feedback on the reaction cycle, which can result in non-linear behavior. In Section 5, we demonstrate that carbodiimide-driven reaction cycles can be used to power molecular machines.

2. Design considerations for carbodiimide-driven reaction cycles

In the following section, we describe how the energy released by the hydration of carbodiimides can transiently activate precursors. We first describe the structure and reaction sequence of carbodiimide-driven reaction cycles. After that, we provide generic design considerations, *e.g.*, selecting the appropriate fuel, nucleophile, and buffer.

In all carbodiimide-driven reaction cycles described in this feature article, the net reaction is the hydration of a carbodiimide, *i.e.*, the reaction of one molecule of carbodiimide-based fuel with one molecule of water to yield its corresponding urea (Fig. 2A). Through the catalytic reaction cycle, the chemical potential of this reaction can temporarily change the function of the catalyst. In the cycle, a carboxylate-carrying precursor (the catalyst) is activated by the carbodiimide and forms the highly reactive intermediate *O*-acylisourea, which is converted to the activated state of the precursor (product) by an inter- or intramolecular attack of a second nucleophile (Fig. 2B). The attack of the nucleophile releases the urea waste product. The activated state is short-lived and, through reaction with water, reverts to the original precursor state. The unaltered precursor can now undergo another cycle of activation and deactivation.

2.1. Design considerations of carbodiimide-fueled reaction cycles

1. Role of fuel. An important factor to consider for carbodiimide-driven reaction cycles is the fuel. In these reaction cycles, the fuel serves as an energy supply but is not part of the activated product. That is unlike ATP-driven phosphorylation where part of the fuel (the phosphate-group) is transiently transferred. Carbodiimides have a relatively low uncatalyzed reactivity and high stability in water, which facilitates storage. For example, EDC has a half-life of roughly 37 h in water at pH7.[18] Due to the difference in hydrophobicity of commercially

 This journal is © The Royal Society of Chemistry 2022

Published on 23 December 2021. Downloaded by Technical University of Munich on 2/3/2022 3:20:27 PM.

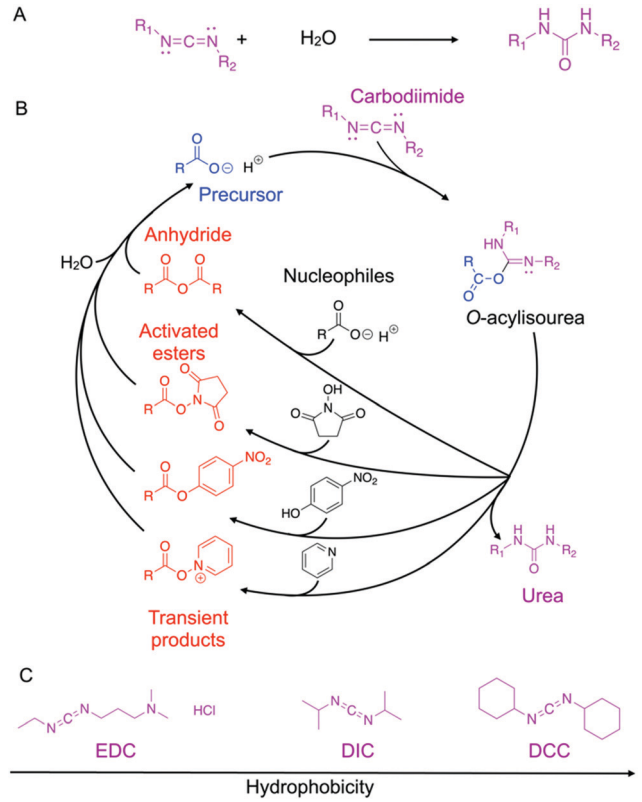

Fig. 2 Carbodiimide-driven reaction cycles. (A) The net reaction: The hydration of the carbodiimide. (B) Schematic representation of a carbodiimide-driven reaction cycle. (C) Standard and commercially available carbodiimides 1-ethyl-3-(3-dimethyl-aminopropyl)carbodiimide hydrochloride (EDC), diisopropylcarbodiimide (DIC) and dicyclohexylcarbodiimide (DCC) were ordered by their hydrophobicity.

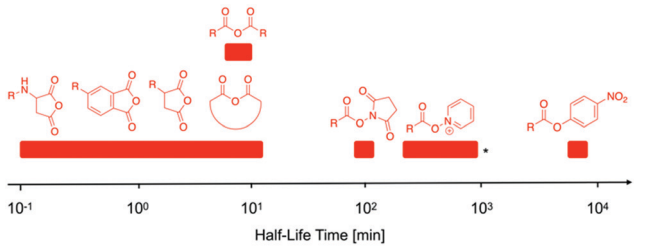

Scheme 1 Half-life times of transient intramolecular anhydrides,[19,23] intermolecular anhydrides,[24] NHS-esters,[20] pyridinium esters* (in 9 : 1 ACN/water mixture),[25] and nitrophenol esters.[21]

available carbodiimides, one can select the appropriate fuel for the solvent in which the carbodiimide-driven reaction cycle operates, *e.g.*, EDC has a good water-solubility whereas DIC and DCC can be applied in organic solvents or mixtures of organic solvent and water (Fig. 2C).[18a] However, EDC is mostly chosen as fuel because most carbodiimide-driven reaction cycles operate in an aqueous solution.

2. Role of the half-life of the product. The half-life of the transient product is critical in the behavior of the catalytic reaction cycle. Short half-lives may be favorable for fast actions in molecular machines. In contrast, longer half-lives may be needed for molecules to nucleate into a molecular assembly. In the case of the carbodiimide-driven reaction cycle, this half-life can be tuned over several orders of magnitude by the nature of the active product. In most published studies, the evolution of the reaction cycle to a batch of carbodiimide-based fuel is reported. By kinetic models, the deactivation rate constants (k_{-1}) can be predicted from which the half-lifes can be calculated by $t_{1/2} = \ln(2)/k_{-1}$. In Scheme 1, we list the half-lives of several active products described in the recent literature. It should be noted that the half-life varies somewhat with the pH. However, given that the activation reaction is strongly pH-dependent and has an optimum around pH 4, the range of pH-values that is used is relatively narrow (*i.e.*, pH 3.5 to 7.4). The transient product with the shortest half-life described in a carbodiimide fueled reaction cycle so far was the aspartic anhydride of the tripeptide Fmoc-AVD with a half-life of roughly 18 s.[19] In contrast, NHS esters have half-lives in the 200–300 min range,[20] and *p*-nitrophenol esters are relatively stable with half-lives of 350 h.[21] The latter's stability offers the possibility to catalyze the deactivation through self-assembly, a process referred to as feedback by catalysis, which we will discuss in Section 4.3.[22]

3. Role of the pH and buffer. In all the studies we found that the rate-determining step of the activation is the formation of the intermediate *O*-acylisourea. This first step occurs in an optimal pH range between pH 3.5 and 4.5.[26] However, as the subsequent attack of a nucleophile requires ionized nucleophiles, it is advisable to choose a pH range above the pK_a of the nucleophile, *e.g.*, at pH 6 for a carboxylic acid nucleophile. A buffer is necessary to maintain a stable pH as protons from the solvent are required to operate the reaction cycle (see Fig. 2).

4. Side products. The formation of side products is a serious concern in the design of a chemical reaction cycle. Where a yield of 99% is spectacular in organic chemistry, it would be disastrous in a chemical reaction cycle. To put that in perspective, if a 100-fold excess of fuel is applied to a precursor, a 1% side reaction would imply that after all fuel is consumed, over 60% of the precursor was converted into the side product.

The common side-reaction in the carbodiimide fueled reaction cycle is the conversion of the reactive intermediate *O*-acylisourea into its corresponding *N*-acylisourea.[27] This first-order side-reaction can be prevented by ensuring that the *O*-acylisourea is as short-lived as possible. In other words, the concentration of the second nucleophile should be as high as possible to ensure there is always a sufficient amount available to immediately attack the *O*-acylisourea after its formation. Side product formation is significantly lower for precursors with a nucleophilic group in proximity to the activated carboxylate that can attack the activated carboxylate intramolecularly compared to precursors that rely on an intermolecular nucleophile. For example, for succinic acid or aspartic acid derivatives, no *N*-acylisourea was observed.[19,28] However, if the distance to the nucleophilic group is large, oligomerization competes with the intramolecular reaction, *e.g.*, for macrocycles.[29]

Published on 23 December 2021. Downloaded by Technical University of Munich on 2/3/2022 3:20:27 PM.

For intermolecular reactions, the side product formation of *N*-acylisourea becomes much more dominant but can be suppressed by catalytic amounts of additional reagents, *e.g.*, pyridine or DMAP.[30]

5. Methods of analysis. The reaction cycle is well-understood and simple to analyze by high-performance liquid chromatography (HPLC) and ^{1}H-nuclear magnetic resonance spectroscopy (^{1}H-NMR). We and others use time-resolved HPLC to quantify the concentrations of each reactant in the reaction cycle. Moreover, time-resolved ^{1}H-NMR can quantify the amount of precursor and product in the self-assembled state. This quantification is based on the NMR silence of self-assembled molecules due to a reduced transversal relaxation time (T_2) that results in signal broadening and loss.[31] Furthermore, we developed an effective method to quench carbodiimide-driven reaction cycles that ends all reactions instantaneously facilitating the analysis of the transient products.[32] This quenching method also enables the automated analysis of the reaction cycle, *e.g.*, by pipetting robots. After the quantification, the respective concentrations can be accurately predicted by kinetic models using MATLAB and Python codes that are commonly accessible.[33] We refer the reader to a review from our group for further reading on the characterization of carbodiimide-driven reaction cycles.[34]

6. Outlook. When designed correctly, the carbodiimide-fueled reaction cycle is robust and functional in a relatively wide range of temperature and pH.[28] It is versatile in both the types of precursors and fuels that can be used. Moreover, the reaction cycle is simple to analyze and well-understood because it can be quenched by an effective method that ends all reactions instantaneously and kinetic models that accurately predict the respective concentrations.[32,33] The reagents are cheap and commercially available and the reaction cycle can easily be tuned by altering the structure of the precursor and/or nucleophile.

3. Carbodiimide-hydration to regulate the folding of molecules

For their catalytic activity, enzymes must be folded in a three-dimensional structure that brings key functional groups in proximity and enables selective interaction with their substrate.[1] A variety of pathological conditions are caused if proteins misfold or fail to remain correctly folded.[35] To regulate protein folding, biology frequently uses energy from chemical fuels for post-translational modifications of proteins, *e.g.*, by phosphorylation and dephosphorylation.[8,36] In the following section, we highlight examples where the transduced energy of carbodiimide-driven reaction cycles is used to drive behavior reminiscent of folding processes in biology, *e.g.*, to alter the three-dimensional structure of molecules in response to chemical fuel. We discriminate folding through single-point and multi-point activation. Folding through single-point activation implies that it is induced by the activation of a single reactive site. Such regulation means that the molecules constantly fold and unfold when fuel is supplied to the system. In contrast, several sites in a molecule have to be activated when folding is induced by multi-point activation. *Vice versa*, this means that if a site deactivates, unfolding does not immediately take place. Unfolding can only be expected when several reactive sites are deactivated, *i.e.*, when the reaction cycle runs low on fuel.

3.1. Folding through multi-point activation

An example of folding through multi-point activation is the transient coil-helix transition of poly-L-glutamic acid (PLG) in an EDC-driven reaction cycle reported by Zhang *et al.* (Fig. 3A).[37] The PLG precursor adopts a random coil conformation in an aqueous solution of buffer and NHS. Upon application of EDC as fuel, the carboxylate moieties are partly converted into their corresponding NHS-esters, which negate the charge repulsion between the carboxylates allowing for α-helix formation of the polypeptide (Fig. 3B). While the NHS-esters along the polypeptide are continuously deactivated through hydrolysis, the chain does not unfold because the peptide remains activated to a large degree. However, when the system runs out of fuel, the deactivation dominates over the activation and, when the majority of the NHS-esters is deactivated, the original random coil conformation is restored. This example shows the power of folding through multi-point activation as the polypeptide remains folded throughout the majority of the cycle. A similar example was reported by Walther *et al.*, who fueled polymethacrylic acid (PMAA) microgels, *i.e.*, micron-sized colloids comprised of a crosslinked poly(2,2,2,-tri-fluoroethyl methacrylate core (PTFEMA) and a PMAA-based shell, with EDC which resulted in temporary deswelling of the particles due to the hydrophobization of the polymer upon activation into the anhydride.[38]

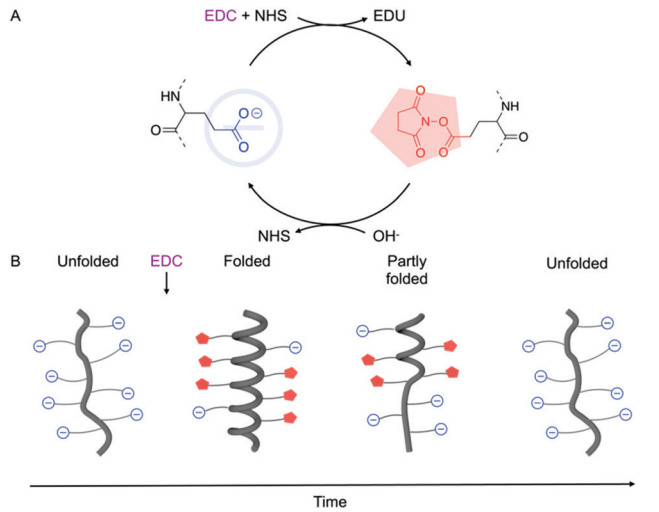

Fig. 3 Carbodiimide-driven folding based on multi-point activation. (A) Reaction cycle of poly-L-glutamic acid (PLG) upon fueling with EDC and addition of NHS-OH. (B) Schematic representation of the temporal course of the folding state of poly-L-glutamic acid (PLG) upon addition of EDC and NHS-OH. Figure adapted from ref. 37 by permission of Elsevier Ltd, Copyright © 2021.

 This journal is © The Royal Society of Chemistry 2022

Published on 23 December 2021. Downloaded by Technical University of Munich on 2/3/2022 3:20:27 PM.

Throughout the deactivation, the microgels reswell and restore the original geometry.

3.2. Folding through single-point activation

In contrast to folding through multi-point activation, single-point activation requires only the activation of a single group on the precursor to induce folding. This means that a molecule folds rapidly after activation, but also immediately unfolds after deactivation. An example of such folding was demonstrated by Hartley *et al.* who used the activation of a diphenic acid-based precursor into its corresponding anhydride through EDC to transiently change the geometry of the molecule, *i.e.*, to transiently fold the molecule.[24b] That activation drastically decreased the torsion angle between the two phenyl rings from 82° to 37°. The geometry change upon fuel addition was transient as deactivation restored the original torsion angle of 82° (Fig. 4A). In other words, the original folding state is restored as soon as the anhydride hydrolyzes back to the initial diphenic acid-based precursor. We envision that the transient change in the torsion angle could be used to control the catalytic activity of a molecule, *e.g.*, by bringing catalytically active substituents in the opposite *meta*-positions of the aromatic rings in proximity due to the folding. Like proteins that are only functional when correctly folded, Hartley *et al.* also demonstrated that carbodiimide fuels can create functional products from non-functional precursors. They reported the EDC-driven formation of functional macrocycles and cages comprised of one or two transient bonds, which can serve as supramolecular hosts for cationic guests.[29,39]

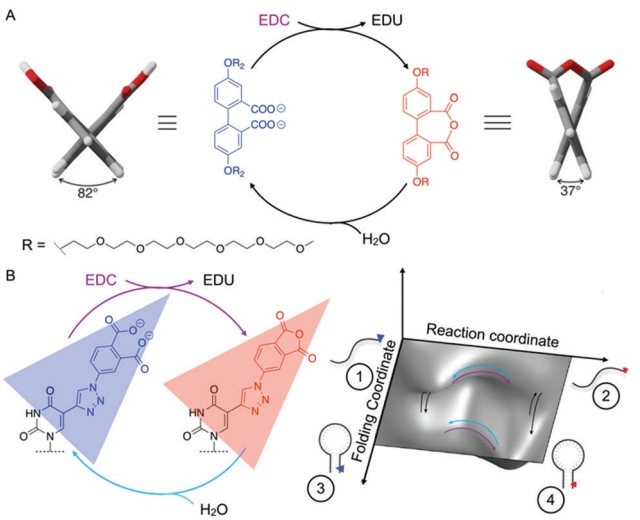

Fig. 4 Carbodiimide-driven folding based on single-point activation. (A) Transient geometry changes of diphenic acid upon addition of EDC. Adapted with permission from ref. 24*b*, Copyright © 2021 American Chemical Society. (B) Schematic representation of the carbodiimide-driven activation and deactivation of a modified thymine precursor on a single-stranded DNA strand. The DNA strand has four different positions in the energy landscape: unactivated and unfolded (1), activated and unfolded (2), unactivated and folded (3), and activated and folded (4). The chemical fueling makes folding in a hairpin more favorable. Figure adapted from ref. 40.

Our group used single-point activation in an EDC-driven reaction cycle to alter the likelihood of folding a DNA hairpin. We used a single-stranded DNA strand that had a high propensity to fold into a hairpin. We mutated one thymine on the hairpin with a modified thymine base that has two negatively charged carboxylates (Fig. 4B). The modification of the thymine destabilizes the hairpin, thereby making it less favorable to fold. Upon activation into the anhydride, the negative charges are negated, and the thymine becomes more rigid which decreases its steric hindrance, electrostatic repulsion and increases its ability to base stack upon folding. Indeed, the propensity of the activated state to fold was restored, and we found that the activated population was mostly in its folded state. The application of chemical energy thus activates a single point of the strand which, induces its partial folding. Unlike the example described above, the picture is more complicated, as the activated molecule can unfold. Essentially, single-point activation of the precursor shifts the equilibrium position between folding and unfolding in favor of the folded state. This concept is best described in an energy landscape (Fig. 4B). The single-stranded DNA can toggle between four states in such an energy landscape: unactivated and unfolded (1), activated and unfolded (2), unactivated and folded (3), and activated and folded (4). The activation by a carbodiimide drives the formation of (2) and (4) and thus makes folding more favorable. However, the folding remains very dynamic, as the equilibrium position is immediately shifted towards the unfolded state when deactivation restores the initial precursor.

4. Carbodiimide-hydration to regulate molecular assemblies

In biological systems, structure formation and self-assembly mostly rely on the continuous consumption of energy and are thus regulated by kinetics rather than by thermodynamics. The dependence on energy derived from chemical fuels might seem wasteful but gives biological systems properties like temporal and spatial control, adaptability, and the ability to self-heal. These properties can be achieved in synthetic systems when we regulate molecular assemblies by synthetic reaction cycles like carbodiimide-driven cycles. In this section, we demonstrate how reaction cycles that catalyze the hydration of carbodiimides have been used to regulate the self-assembly or phase separation of molecules to yield compartments. Compartmentalization is considered a crucial characteristic of living systems, and theoretical calculations revealed that complex behavior can be observed when compartmentalization is indeed regulated by chemical reactions, which include the suppression of Ostwald ripening[41] and even compartment self-division without the need of complex molecules.[42] Moreover, we show how these catalytic reaction cycles can regulate the self-assembly of networks of fibers reminiscent of the cytoskeleton. Biology not only controls the self-assembly of its components by reaction cycles but also regulates these reaction cycles by so-called feedback mechanisms, *e.g.*, the assembly accelerates or decelerates a reaction of the reaction cycle

Published on 23 December 2021. Downloaded by Technical University of Munich on 2/3/2022 3:20:27 PM.

and thus regulates its own activity. We close the section by showing recent examples of carbodiimide-driven assemblies that exert feedback on their own reaction cycle.

4.1. Compartments

The contemporary cell is a complex microenvironment in which countless reaction cycles take place simultaneously. Compartments avoid mutual interferences between these reactions. They can also control the influx and outflux of molecules thereby up- or down-concentrating reactants and modulating biocatalytic efficiency. Since compartmentalization is a fundamental principle of all forms of life, it likely played an essential role in its emergence, as so-called protocells.[43] Thus, numerous models have been developed to better understand how these compartments could have emerged and performed metabolic and replication functions. On the one hand, self-assembly of amphiphiles into vesicles is considered as protocell model.[43] However, these compartments show limitations when considering a prebiotic scenario, *e.g.*, the lack of permeability to many solutes, which requires complex enzyme machinery to control the flux of molecules. Trying to overcome such limitations, other types of compartments have been suggested as protocell models. Among them, more permeable fatty acid vesicles,[44] micelles,[45] and membranelles compartments like liquid–liquid phase-separated droplets and complex coacervate droplets have been studied.[46] Although the field has successfully evolved in complexity,[47] most of these models exist under thermodynamic conditions and, thus, do not reflect the properties of the dynamic compartments found in biology.

Recently, several synthetic compartments regulated through chemical reactions have been reported in the literature.[11c,12d] In some cases, the works demonstrated unique properties that could not be observed in equilibrium or close to equilibrium systems which include self-replication[12d] or the formation of compartments that act as nanoreactors.[11c] In the following paragraphs, we will describe several examples of compartments formed at the expense of carbodiimide fuels. We will highlight how important it is to kinetically control the formation and collapse of these synthetic compartments to achieve unique properties not observed in equilibrium systems.

We described an interesting new behavior in chemically fueled phase-separated oil droplets, which is a direct result of its chemically fueled nature (Fig. 5A and B).[23] The active droplets we created ripen exceptionally quick, meaning orders of magnitude faster than expected for Ostwald ripening.[48] In this context, ripening means the growth of large droplets at the expense of small ones. This ripening is observed in passive systems and is driven by the tendency of a system to decrease its interfacial surface area, *i.e.*, to reduce the total interfacial surface area, the system favors one large droplet over many small ones.

When the system was fueled with a single batch, we made the surprising observation that the average droplet volume increased continuously throughout most of the experiment (Fig. 5C, top row). Towards the end of the cycle, the droplet volume quickly decreased, and the droplets disappeared.

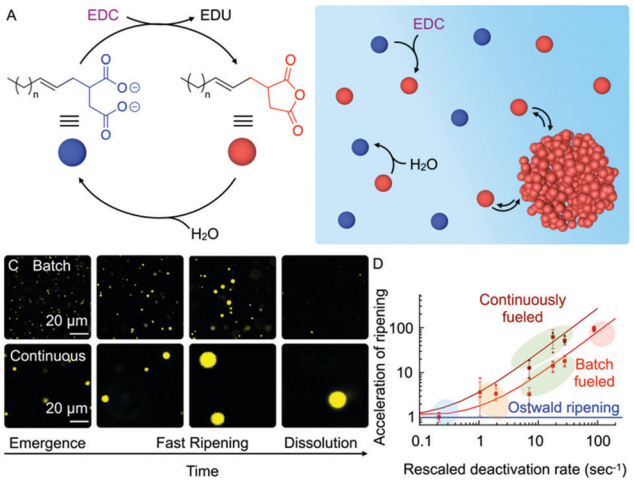

Fig. 5 Accelerated ripening in carbodiimide-driven reaction cycles. (A) EDC-driven reaction cycle of a succinate derivative. (B) Schematic representation of the hydrophobic products that phase-separate into droplets after consumption of the fuel. The products are deactivated in water and return to the initial precursor form. (C) Confocal micrographs of the batch- and continuously fueled droplets over time. (D) Acceleration of ripening as a function of the deactivation rate for different molecules. Lines represent the theoretical predictions while squares represent average values of experimental data (n = 3). Colored areas stand for the four different reaction cycles. (C) and (D) adapted from ref. 23 by permission from Wiley-VCH GmbH., Copyright © 2020.

Moreover, when experiments were sustained out of equilibrium by the constant supply of chemical fuel, the ripening was further accelerated (Fig. 5C, bottom row). Furthermore, for all the chemical reaction cycles used, the average volume's growth rate was faster than Ostwald ripening. More striking was the relation between the reaction rate of deactivation and the ripening rate, *i.e.*, the faster the deactivation, the faster the ripening. (Fig. 5D).

The mechanism for the ripening is based on a combination of Ostwald ripening and the kinetics of the fuel-driven reaction cycle. Ostwald ripening creates a concentration gradient from small to large droplets leading to a diffusion-limited flux of droplet material. On top of that, the reaction cycle creates local over- and undersaturation in the aqueous solution between the droplets through local activation and deactivation, respectively. The undersaturation tends to remove material from small droplets, whereas the activation tends to add material to the large droplets. For this mechanism, it is thus crucial that activation and deactivation occur between the droplets.

We also developed a different type of chemically fueled droplets, in which activation predominantly happens outside of the droplets whereas deactivation happens mostly inside of the droplets.[49] These droplets are based on complex coacervation between a peptide and RNA (polyU). The affinity of the peptide towards the RNA is controlled by the carbodiimide-fueled chemical reaction cycle (Fig. 6A and B). By using a zwitterionic peptide as a precursor, the activation renders the peptide cationic and thus increases its affinity for RNA. When a sufficient amount of peptide is activated, it phase-separates

 This journal is © The Royal Society of Chemistry 2022

Published on 23 December 2021. Downloaded by Technical University of Munich on 2/3/2022 3:20:27 PM.

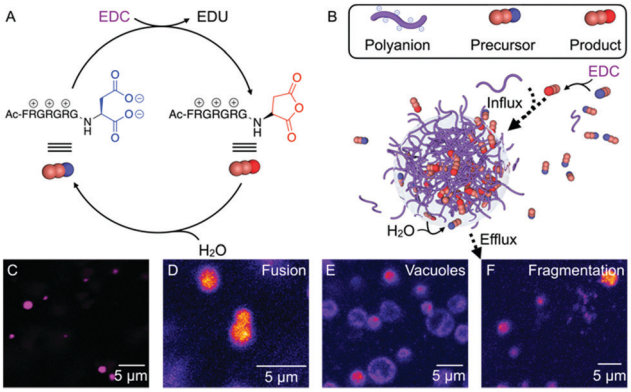

Fig. 6 Carbodiimide-driven complex coacervation. (A) Schematic representation of the EDC-driven reaction cycle of an Ac-F(RG)$_3$D-OH precursor. F stands for phenylalanine, R stands for arginine and G stands for glycine. (B) Schematic representation of an EDC-driven complex coacervate between a positively charged peptide (product) and a polyanion (RNA). Figure (A) and (B) adapted from ref. 50, Copyright © 2021 American Chemical Society. (C) Confocal microscopy picture of complex coacervates. (D) Confocal microscopy picture of a fusion event between two complex coacervates. (E) Confocal microscopy picture showing the formation of vacuoles. (F) Confocal microscopy picture of fragmentation events. Micrographs adapted from ref. 49 by permission from Springer Nature Ltd., Copyright © 2020.

with the RNA resulting in droplet formation (Fig. 6B and C). Indeed, the complex coacervate-based droplets form spontaneously and decay in the absence of fuel. Unlike the oil-based droplets we described above, these droplets remain hydrated, and deactivation can thus take place within the droplets. This internal deactivation results in unique behaviors. For example, we observed fusion events between complex coacervates (Fig. 6D), the formation of vacuoles (Fig. 6E), and the collapse into fragments towards the end of the cycle (Fig. 6F).

A further study demonstrated that droplet formation was not limited to RNA as polyanion, but poly(styrenesulfonate)-PSS) and di- or triblock copolymers of PSS with poly(ethylene glycol) (PEG) as a repulsive block could also form droplets. Moreover, the morphology of the phase-separated structures could be tuned by the type of polyanion used. These findings enabled us to suggest heuristic design rules for chemically fueled complex coacervate-based assemblies.[50]

Examples of vesicles formed by a chemical reaction cycle remain scarce despite their relevance as compartments in biology. One of the few examples of fuel-driven self-assembled vesicles was based on surfactants that interact with adenosine triphosphate (ATP) to form vesicles.[11c] Their lifetime could be regulated by the amount of ATP and the vesicles acted as nanoreactors but only as long as the fuel was present. Chemically fueled vesicles that use carbodiimide as a fuel also exist.[51] Here, the authors reported the chemically fueled self-assembly of synthetic vesicles driven by the energy gained from the hydrolysis of EDC. In particular, the functional moiety from the precursor, aspartic acid (Fmoc-GGD) or glutamic acid (Fmoc-GGE) reacted with the fuel and formed the corresponding anhydrides, which have a lower solubility and therefore, self-assembled into vesicles. The lifetime of the transient vesicles could be regulated by the amount of EDC. Interestingly, the work highlighted the importance of charge balancing to create stable membranes. In this case, the precise co-assembly between precursor and product made the membrane formation possible. In dynamic vesicles, the chemical reaction cycle and the assembly and disassembly process are tightly connected. This means that the vesicles evolve dynamically through the whole cycle, in other words, they are continuously remodeled. Such behavior is reminiscent of vesicles found in biology and therefore, we envisioned them as suitable models for membrane vesicular compartments.

Micellar compartments have been extensively used as nanoreactors as they represent one of the easiest ways to achieve catalysis in water.[52] The simplicity of these micellar compartments as catalysts comes also with disadvantages, *e.g.*, the low amounts of substrate that can be incorporated and the inhibition of the catalytic effect due to the accumulation of the product. The incorporation of a chemical reaction cycle that drives the assembly and disassembly of micellar compartments can overcome some of these issues as already pointed out in recent literature.[53] For example, Yuan and coworkers reported the formation of carbodiimide-driven micelles using a block copolymer based on poly(ethylene glycol) and polyacrylic acid (Fig. 7A and B).[53a] Upon addition of fuel (EDC) and a second nucleophile like *N*-hydroxysuccinimide, an activated ester was formed with a lower solubility than its precursor driving the formation of micelles. Due to the deactivation, the micelles were present as long as fuel was available. The lifetime of the micellar solution could thus be tuned by the amount of fuel, and the amount and nature of the second nucleophile. These micelles were used as nanoreactors to catalyze the dimerization

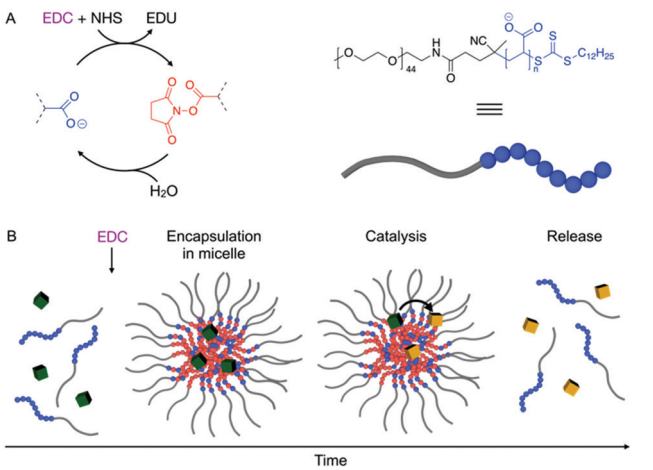

Fig. 7 Carbodiimide-driven self-assembly of micellar nanoreactors. (A) Reaction cycle and structure of a PEG$_{45}$-*b*-PAA$_{78}$ precursor fueled with EDC and *N*-Hydroxysuccinimide (NHS) (B) schematic representation of the temporal course of fueling a PEG$_{45}$-*b*-PAA$_{78}$ block copolymer with EDC. The fuel addition decreases the electrostatic repulsion in the PAA-block which results in transient formation of micelles. The micelles are used as transient nanoreactors that up-concentrate hydrophobic molecules on the interior. The catalytic products are spontaneously released when the micelles disappear due to fuel depletion. Figure adapted from ref. 53*a* by permission from The Royal Society of Chemistry, Copyright © 2021.

Published on 23 December 2021. Downloaded by Technical University of Munich on 2/3/2022 3:20:27 PM.

of anthracene mediated by UV light. A similar molecular design was reported by the Walther and our group.[53b] In this particular case, the authors showed the formation of transient micelles by using a block copolymer that comprises a hydrophilic poly(ethylene glycol) and a poly(styrene-*alt*-maleic acid) block. The addition of EDC allowed the formation of an intramolecular anhydride and consequently, due to the charge abolishment, the micelles were formed. In this case, the micelles were used as nanoreactors to catalyze Diels–Alder reactions between hydrophobic substrates, which were able to partition inside the micelles. Importantly, the temporary nature of these micellar nanoreactors avoided in both cases the product inhibition because the product was spontaneously released when the micelles dissolved. This particular feature of fuel-driven micelles cannot be achieved when regulated by thermodynamics.

4.2. Fiber networks

The cytoskeleton is a network of filamentous assemblies and regulatory proteins that controls the intracellular transport, the active movement of the cell, and mechanically stabilizes the cell against deformation.[54] The network comprises microtubules, actin, filaments, and intermediate filaments which are tightly regulated by the cell using energy that is transduced from ATP or GTP hydrolysis.[55] The dependence of polymerization on a chemical fuel enables biological systems to temporally and spatially control the self-assembly of the cytoskeleton. These dynamic properties and functions of these networks make them exciting for the development of smart and responsive materials.

Like the ATP- and GTP-driven assembly of the cytoskeleton, self-assembled fiber networks can also be formed in carbodiimide-driven reaction cycles.

We identified that, until now, three different strategies have been used to create networks in carbodiimide-driven reaction cycles. The first strategy is based on the abolishment of the negative charges on an aspartic acid precursor due to the anhydride formation upon the addition of a carbodiimide fuel. The charge abolishment significantly decreases the repulsive interactions between the molecules and thus drives the self-assembly. We demonstrated, for example, that an Ac-FIID-OH precursor forms self-assembled peptide fibers and transient hydrogels upon applying EDC (Fig. 8A and B).[56] We showed that the self-assembly behavior can be controlled by the tuning of the attractive and repulsive interactions between the precursors and products by molecular design and salt addition. A detailed study showed that deactivation occurs both on the fibers and in the solution (Fig. 8C). However, deactivated precursor in the fiber did not immediately disassemble from the fiber which means that these fibers are comprised of co-assembled product and precursor.

Another strategy to form self-assembled fiber networks is based on linking two non-assembling precursors. For example, Haldar *et al.* showed that a Cbz-F-OH precursor forms a symmetric anhydride product with another precursor molecule upon addition of EDC (Fig. 8D).[57] The symmetric anhydride

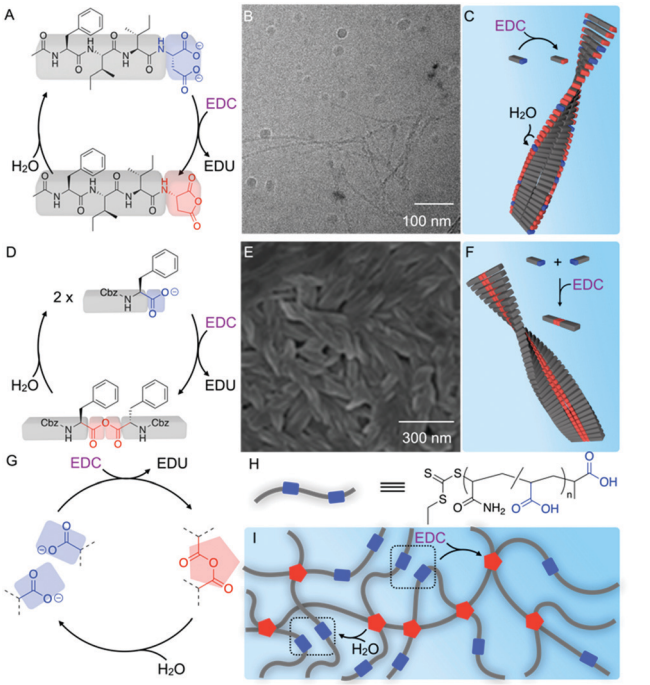

Fig. 8 Three different strategies to form self-assembled fiber networks in carbodiimide-driven reaction cycles. (A) Transient charge abolishment of an Ac-FIID-OH precursor due to the anhydride formation upon addition of EDC. (B) Cryo-TEM micrograph of self-assembled Ac-FIID-OH fibers fueled by EDC. Micrograph reproduced from ref. 56, Copyright © 2020 American Chemical Society. (C) Schematic representation of self-assembled Ac-FIID-OH fibers fueled by EDC. (D) Linking of two non-assembling Cbz-F-OH precursors upon addition of EDC to form the self-assembling symmetric anhydride product. (E) FE-SEM micrograph of self-assembled Cbz-F-OH fibers fueled by EDC. Micrograph reproduced from ref. 57 by permission from The Royal Society of Chemistry, Copyright © 2021. (F) Schematic representation of self-assembled Cbz-F-OH fibers fueled by EDC. (G) Schematic representation of the cross-linking of acrylic acid (AA) polymers in an EDC-driven reaction cycle. (H) Molecular structure of the poly(Am-*r*-AA) precursor. Adapted from ref. 58 by permission from The Royal Society of Chemistry, Copyright © 2019. (I) Schematic representation of the crosslinked network formed by the poly(Am-*r*-AA) precursor in an EDC-driven reaction cycle. Figure adapted from ref. 59 by permission of Elsevier Ltd., Copyright © 2021.

forms a fiber network which results in transient hydrogel formation (Fig. 8E and F). Adams *et al.* used a similar strategy for a gel-to-gel transition of an amphiphilic precursor that forms a hydrogel with needle-like structures in the absence of EDC. Upon fuel addition, the morphology of the gel changed to net-like fiber arrangements which also results in an improved mechanical strength compared to the initial precursor gel.

The third strategy to induce transient self-assembly of a fiber network by a carbodiimide fuel is based on cross-linking of polymeric precursors. Konkolewicz *et al.* were the first to report a transient hydrogel formation upon cross-linking of different acrylamide (Am)-*r*-acrylic acid (AA) copolymers with EDC (Fig. 8G–I).[58] Moreover, the stiffness and lifetime of the hydrogel can be tuned by the ratio of Am:AA because increasing the AA fraction increases the number of crosslinks.[60] Wang *et al.* used a similar PNIPAm-*co*-AA copolymer that formed a transient

 This journal is © The Royal Society of Chemistry 2022

Published on 23 December 2021. Downloaded by Technical University of Munich on 2/3/2022 3:20:27 PM.

hydrogel due to cross-linking of the polymer strands upon addition of EDC.[59] Excitingly, the study demonstrated that the chemically fueled hydrogel can control the crystal growth of pharmaceutical model drugs, such as carbamazepine (CBZ). The transient hydrogel enables to control the size of the crystals by adjusting the initial amount of fuel. In general, higher fuel concentrations resulted in the formation of denser networks and higher lifetimes which accelerated the nucleation of CBZ. Moreover, the transient nature of the hydrogel offers the advantage that crystals can be released upon degradation of the hydrogels, *i.e.*, without product inhibition. Another example for cross-linking by a carbodiimide fuel is reported by Cheng and coworkers who used a tetraphenylethylene precursor with multiple carboxylic acids that are crosslinked upon the addition of EDC. The anhydride formation resulted in aggregation and transient hydrogel formation which enabled them to apply the transient hydrogel as writable and self-erasable material.[61]

4.3. Feedback mechanisms in carbodiimide-fueled assemblies

In the previous sections, we described that carbodiimide-driven reaction cycles can regulate molecular self-assembly yielding temporary and dynamic structures with properties that are not observed in equilibrium. However, more sophisticated behavior can be observed when assemblies exert feedback on their activation or deactivation. For example, such reciprocal coupling between structure formation and reaction cycle can give rise to oscillations, pattern formation, hysteresis, and bistability. Assemblies can exert feedback on their reaction cycle by changing the rate of activation or deactivation. Moreover, feedback can either be positive or negative depending on whether the assembly accelerates or decelerates the reaction. Thus, four modes of feedback are possible: the assembly exerts positive feedback (accelerates) on its activation, it exerts negative feedback (decelerates) on its activation, it exerts positive feedback on its deactivation, or it exerts negative feedback on its activation (Scheme 2). Two of these mechanisms increase the amount of activated product, *i.e.*, obviously the positive feedback on activation (which one could refer to as "autocatalysis"), but also the negative feedback on the deactivation, which we have referred to as "self-protection". The other two feedback mechanisms decrease the amount of activated product, *i.e.*, negative feedback on activation and the positive feedback on deactivation (which we refer to as "self-destruction").

We found two generalizable mechanisms by which the assemblies regulate their carbodiimide-driven reaction cycle, *i.e.*, either the assembly changes the local concentration of reagents required in the activation or deactivation, or the assembly changes the microenvironment of the precursor or product thereby lowering the activation energy of a reaction in the cycle. A rate of a reaction depends on two components, *i.e.*, the rate constant and the concentration of the involved reagents. Broadly speaking, the first mechanism (up- or down-concentration) affects the concentration to alter the reaction rate, whereas the second mechanism affects the rate constant by lowering the activation energy.

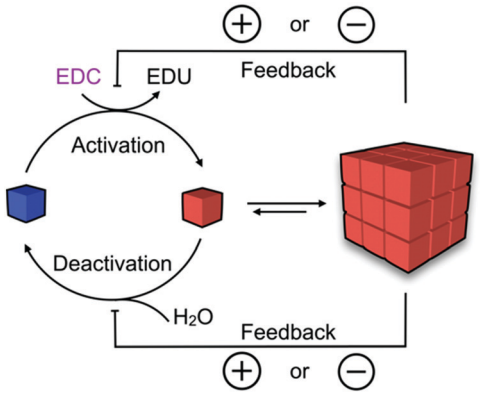

Scheme 2 Possible feedback of the assembly on its chemically fueled reaction cycles.

The assembly up- or down-concentrates reactants. Assemblies can partition or exclude certain molecules through co-assembly or co-phase separation. Consequently, the concentration of these molecules is increased or decreased within the assembly, respectively. We refer to this as up- or down-concentration. If the up- or down-concentrated molecule is a reactant in the cycle, the process will change the rate in which this reactant is involved.[62] This feedback mechanism has been observed in other systems, *e.g.*, the autocatalytic formation of micelles, inverse micelles, and vesicles from two phase-separated reagents.[12d,14a,45a,63] In carbodiimide driven reaction cycles, the deactivation always occurs through hydrolysis and thus requires water. This means that a change in the concentration of water compared to the bulk phase will affect the deactivation mechanism. Such a feedback mechanism has been found in phase-separated oil droplets.[64] These oil droplets very drastically down-concentrate the concentration of water. Effectively, no water is present in these oil droplets, which means that the deactivation reaction does not occur inside the droplets (Fig. 9A). In other words, the droplets exert negative feedback on their deactivation and thus protect themselves. Nevertheless, deactivation can still occur at the oil–water interface and in the water phase of the emulsion, when the solubility of the oil is relatively high. Because the exchange at the oil–water interface is fast, a product that is hydrolyzed in the water phase is rapidly replaced by a product from the oil phase. This relation leads to a very characteristic zeroth-order deactivation, *i.e.*, the deactivation reaction is concentration-independent until all product in the droplets is hydrolyzed. This feedback mechanism is a negative feedback on the deactivation (phase separation decelerates the hydrolysis) and is thus a "self-protection" mechanism as the droplets protect their building blocks. Such a self-protection mechanism increases the survival time of phase-separating products which is why phase separation can be used to select certain products over others. When a library of aliphatic acids (precursors) is competing for EDC as fuel, we found that the negative feedback of droplets can increase the survival time of phase-separating, transient anhydride products over others.[24a] In one example, propionic acid (C_3) and hexanoic acid (C_6) competed for EDC (Fig. 9B and C).

Published on 23 December 2021. Downloaded by Technical University of Munich on 2/3/2022 3:20:27 PM.

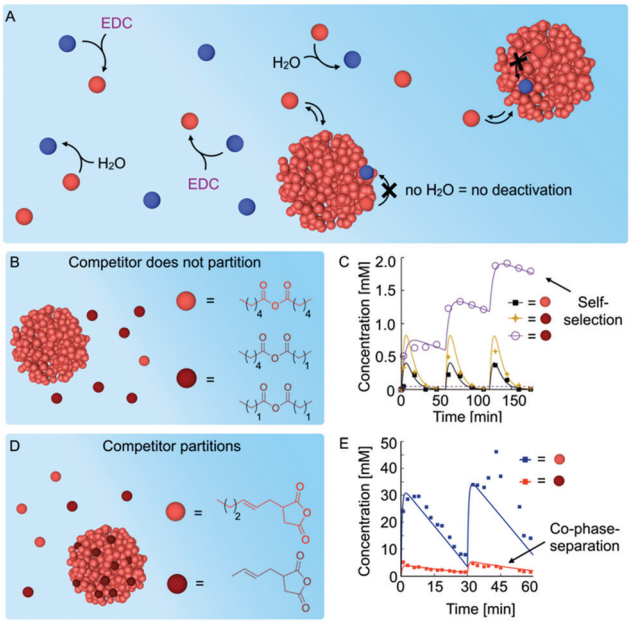

Fig. 9 Self-protection of carbodiimide-fueled anhydride droplets. (A) Schematic representation of the EDC-driven phase separation of anhydride products (red) into droplets which down-concentrate the concentration of water compared to the bulk phase and thus exert negative feedback on the deactivation by hydrolysis. (B) Schematic representation and (C) anhydride concentration profile of propionic acid (C_3) and hexanoic acid (C_6) competing for fuel in an EDC-driven reaction cycle. The self-protection of droplets selects the phase-separating product C_6C_6 over the other competing products (C_3C_3 and C_6C_3). Adapted from ref. 24*a* by permission from Springer Nature Ltd, Copyright © 2018. (D) Schematic representation and (E) anhydride concentration profile of 2-butenylsuccinic acid and 2-hexenylsuccinic acid competing for fuel in an EDC-driven reaction cycle. The soluble product 2-butenylsuccinic anhydride co-phase separates with the insoluble 2-hexenylsuccinic anhydride and exploits the protective environment offered by the host droplets. Adapted from ref. 65 by permission from The Royal Society of Chemistry, Copyright © 2021.

While the soluble anhydride products C_3C_3 and C_3C_6 (dark red) completely hydrolyze in starvation periods without fuel, the phase separation of the droplet-forming C_6C_6 (red) decelerates its deactivation. The self-protection ensures that some anhydride can survive the starvation period.[24a] After several fueling-starvation cycles, the self-protecting C_6C_6 product accumulates. This study demonstrates that in chemically fueled systems, not only autocatalysis, but also self-protection, can result in accumulation.

In another study, we found that the soluble 2-butenylsuccinic anhydride (dark red) can co-phase-separate with droplets formed by the more hydrophobic competitor 2-hexenylsuccinic anhydride (red) and thereby benefit from the self-protection mechanism without being able to phase-separate by itself (Fig. 9D and E).[65] This behavior resembles parasitic behavior in biological systems as both reaction cycles are competing for fuel and the soluble product exploits the protective environment offered by the host droplets.

The self-protection of the anhydride by the droplets results in zeroth-order decay kinetics which can be applied to set free hydrophobic drugs from an emulsion with linear kinetics in a drug-delivery platform.[28] Excitingly, the rate of the release of drugs and the period over which the drugs are released can be pre-programmed by the amount of fuel added.[66] We further extended the feedback regulation of droplets and designed an opposing feedback mechanism that rapidly accelerates the deactivation once a certain threshold is reached.[67] The mechanism is based on the *in situ* formation of micelles by the surfactant precursor which act as a phase-transfer catalyst for the anhydride. In other words, the precursor micelles up-concentrate the anhydride in solution and thus accelerate the hydrolysis. Upon hydrolysis, more precursor is released which further solubilizes the anhydride and accelerates the hydrolysis rate, *i.e.*, a self-immolative decay. This mechanism drastically decreased the time the material switches off, which enabled us to precisely control the material properties in time.

Feedback through catalysis by the assembly. An alternative mechanism in which the assembly accelerates the activation or deactivation is through catalysis, *i.e.*, by lowering the activation energy required for the reaction.[62] Unlike the previous mechanism based on up- or down-concentrating, catalysis always accelerates the reaction, *i.e.*, this feedback mechanism is per definition positive. Nevertheless, the feedback can be on the activation or deactivation. Indeed, Das and coworkers showed an example of positive feedback on deactivation through self-assembly. They used the amino acid histidine in an amphiphile (C18H) that can catalyze the activation and deactivation in EDC-driven reaction cycles.[22b] This catalysis is particularly effective when multiple histidine amino acids come in proximity as expected in an assembly. Upon EDC addition, the C18H is converted to its nitrophenol ester (C18H-NP) which results in rapid gel formation (Fig. 10A). Upon assembly, the histidine derivative catalyzes both the activation and the deactivation. On the one hand, it serves as a base and enables the ester formation of the alcohol and carboxylic acid.

The ester formation is also catalyzed by the non-assembled precursor which means that the catalysis of the activation reaction is not related to self-assembly. On the other hand, the histidine influences the local pH and thus catalyzes the hydrolysis of the relatively stable ester bond. The latter causes disassembly and a gel-to-sol transition. For the catalysis of the deactivation reaction, the self-assembled fiber's microenvironment is crucial as the ester hydrolysis does not occur in the absence of fibers (Fig. 10B).

Moreover, the authors showed that the concept of cooperative catalysis of histidine is transferable to other systems, *e.g.*, amyloid peptides.[22a] Similarly, we found that the hydrophobic microenvironment of self-assembled peptide fibers catalyzes the activation and deactivation reaction in EDC-driven reaction cycles.[31]

5. Outlook. Carbodiimide-hydration to perform work; molecular machines

In the previous section, we showed that self-assembled structures can exert feedback on their regulating chemical reactions

 This journal is © The Royal Society of Chemistry 2022

Published on 23 December 2021. Downloaded by Technical University of Munich on 2/3/2022 3:20:27 PM.

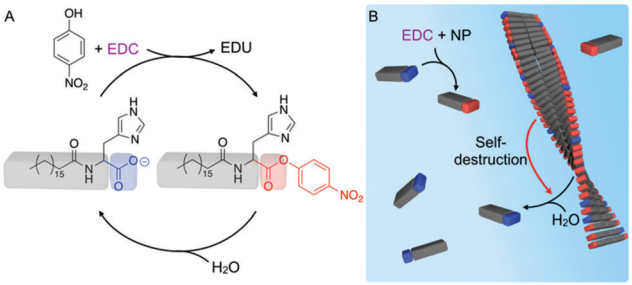

Fig. 10 Feedback by catalysis in carbodiimide-driven reaction cycles. (A) Reaction cycle of C18H fueled with nitrophenol (NP) and EDC resulting in transient formation of C18H-NP. Adapted from ref. 22*b* by permission from the Wiley-VCH Verlag GmbH, Copyright © 2019. (B) Schematic representation of C18H-NP nanofibers catalyzing the hydrolysis of C18H-NP and thus its self-destruction.

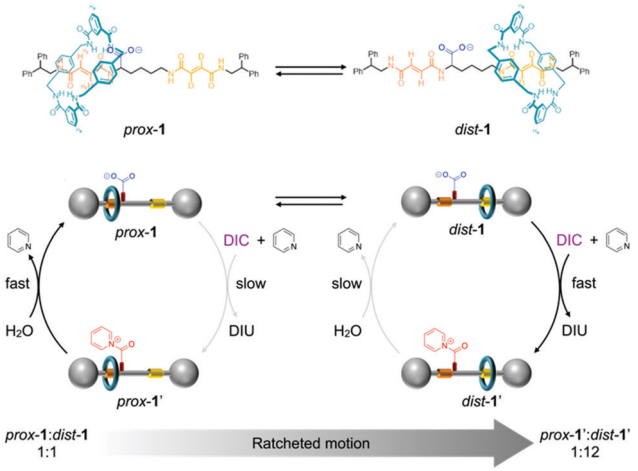

Fig. 11 Molecular machines driven by carbodiimide hydration. A rotaxane precursor with a catalytic carboxylate group reacts with a DIC fuel and pyridine to form a transient activated ester barrier for macrocycle ring movement that hydrolyzes back to the initial precursor. Activation and deactivation are kinetically gated and favor forward stepping of the machine which drives the significant shift from 1 : 1 to 1 : 12 in prox:dist population. Adapted with permission from ref. 25, Copyright © 2021 American Chemical Society.

which can result in self-destruction or self-protection. Moreover, feedback mechanisms are also required to perform work at the expense of chemical fuel, as molecular machines do in biological systems.[68] Biological machines are kinetically gated which means that the rates of activation or deactivation are dependent on the mechanical state of the machine. In other words, through a feedback mechanism, the next step in the chemical reaction cycle is more favorable if the machine has taken its next. In fact, biological machines are usually doubly kinetically gated which means that both fuel-driven activation and the deactivation favor forward-stepping of the machine.[25,69] Most synthetic analogs of molecular machines require sequential additions of various reagents for their operation. Typically, an initial stimulus is added to start the operation of the machine followed by an opposite stimulus that resets the system to its original state, *e.g.*, acid–base chemistry,[70] and ion-binding.[71] This means that in contrast to biological machines, these synthetic machines do not operate autonomously. Up to now, only one synthetic type of an autonomous molecular machine is reported which is driven by a Fmoc-Cl chemical fuel.[72] However, only the fuel addition is kinetically gated for this type of molecular machine which means that the deactivation formation is independent of its mechanical state.[25] Moreover, in contrast to the high efficiency of fuel-to-waste conversion in biological systems, the Fmoc-Cl fuel is prone to decomposition *via* side reactions as only roughly 10% of the fuel is consumed by the machine.[72] Given the stability of carbodiimides, the low susceptibility for side-reactions, the controllability of the reaction cycle, and the deactivation that requires only water, carbodiimide-driven reaction cycles could be ideal for the autonomous operation of synthetic molecular machines. Moreover, carbodiimide-driven reaction cycles are characterized by high catalytic efficiency of 80–90%.[25]

Indeed, Leigh and coworkers used a carbodiimide-driven reaction cycle to drive a molecular information ratchet (Fig. 11).[25] The machine is based on a rotaxane precursor with one carboxylate as catalytic group. It is also functionalized with two fumaramide groups that can bind a benzylic amide macrocycle. These binding sites are on either side of the catalytic group, *i.e.*, relatively close to the catalytic group as the proximal (prox) side and the further distal (dist) side. In the absence of fuel, the macrocycle can move freely between the two binding sites and is distributed more or less evenly. Upon the addition of DIC and pyridine, a transient *N*-acyl pyridinium ion forms which acts as a barrier for the macrocycle movement. Interestingly, the barrier formation changes the ratio of the prox:dist equilibrium population of the macrocycle from roughly 1 : 1 to 1 : 12. The uneven distribution is a result of kinetic gating. The formation of the barrier, *i.e.*, the activation reaction, is two times faster when the macrocycle is locked onto the dist'-site compared to the prox'-site due to its steric hindrance. The deactivation is also kinetically gated. Hydrogen bonds between the macrocycle and the *N*-acyl pyridinium ion increase the hydrolysis rate of the barrier of the prox'-rotaxane by an 8-fold compared to the dist'-rotaxane. In summary, the significant shift in the population of the two binding sites is driven by the kinetic gating of the molecular machine as both reactions favor the population of the dist'-binding site. The hydrolysis of the barrier restores the prox : dist equilibrium population of 1 : 1 after depletion of the fuel.

6. Conclusions

Carbodiimide-driven reaction cycles are promising tools for the bottom-up synthesis of life and the creation of smart, and responsive materials. They have high catalytic efficiency, are robust in terms of temperature and pH, tunable by molecular design, and versatile as any precursor with a catalytic carboxylate moiety can be applied. These reaction cycles can regulate processes that are reminiscent of essential processes in living systems, such as folding, and structure formation. Like their biological role models, they can regulate the self-assembly of

Published on 23 December 2021. Downloaded by Technical University of Munich on 2/3/2022 3:20:27 PM.

synthetic compartments and fiber networks. However, in particular, the synthetic fiber networks are far from the dynamics of the cytoskeleton. In the future, the dynamics of synthetic fiber networks have to be improved to synthesize life-like systems, *e.g.*, by reducing the kinetic trapping of precursors in the fibers. Moreover, carbodiimide-regulated assemblies can also exert feedback on their reaction cycle which can drive the motion of molecular machines and can result in complex behavior, such as self-protection, cooperative catalysis, and self-immolation. So far, carbodiimide-driven assemblies exert feedback by catalysis and up-or down-concentration of reagents. However, feedback of the assembly by self-replication is not yet observed. In the future, designing carbodiimide-driven assemblies such that they serve as a template for their own formation could be a step towards the bottom-up synthesis of life for which self-replication is an essential property. Moreover, finding ways to use the directional changes of components in response to a carbodiimide fuel to perform useful work (a task) could enable the development of life-like molecular machines, *e.g.*, ATPase membrane pumps.

Author contributions

All authors gave approval to the final version.

Conflicts of interest

There are no conflicts to declare.

Acknowledgements

This feature article was composed within the Max Planck School Matter to Life supported by the German Federal Ministry of Education and Research (BMBF) in collaboration with the Max Planck Society. JB, MTS, and PS are grateful for funding by the Deutsche Forschungsgemeinschaft (DFG, German Research Foundation) – SFB-863 – Project ID 111166240 (Project B11). J. B. is grateful for the funding by the European Research Council (ERC starting grant 852187) and the DFG excellence strategy which funds the TUM Innovation Network for Robot Intelligence in the Synthesis of Life (RISE). K. D. thanks the financial support from the China Scholarship Council.

References

1 T. E. Creighton, *Biochem. J.*, 1990, **270**, 1.
2 S. E. Ahnert, J. A. Marsh, H. Hernández, C. V. Robinson and S. A. Teichmann, *Science*, 2015, **350**, aaa2245.
3 J. N. Israelachvili, D. J. Mitchell and B. W. Ninham, *Biochim. Biophys. Acta*, 1977, **470**, 185.
4 V. A. Belyi and M. Muthukumar, *Proc. Natl. Acad. Sci. U. S. A.*, 2006, **103**, 17174.
5 (*a*) V. Ottani, M. Raspanti and A. Ruggeri, *Micron*, 2001, **32**, 251; (*b*) L. E. R. O'Leary, J. A. Fallas, E. L. Bakota, M. K. Kang and J. D. Hartgerink, *Nat. Chem.*, 2011, **3**, 821.
6 (*a*) J. A. Elemans, A. E. Rowan and R. J. Nolte, *J. Mater. Chem.*, 2003, **13**, 2661; (*b*) W. Pfeifer and B. Saccà, *ChemBioChem*, 2016, **17**, 1063; (*c*) B. B. Gerbelli, S. V. Vassiliades, J. E. U. Rojas, J. N. B. D. Pelin, R. S. N. Mancini, W. S. G. Pereira, A. M. Aguilar, M. Venanzi, F. Cavalieri, F. Giuntini and W. A. Alves, *Macromol. Chem. Phys.*, 2019, **220**, 1900085; (*d*) H. M. Keizer and R. P. Sijbesma, *Chem. Soc. Rev.*, 2005, **34**, 226.
7 (*a*) R. Merindol and A. Walther, *Chem. Soc. Rev.*, 2017, **46**, 5588; (*b*) G. Ragazzon and L. J. Prins, *Nat. Nanotechnol.*, 2018, **13**, 882; (*c*) S. De and R. Klajn, *Adv. Mater.*, 2018, **30**, 1706750.
8 A. Bah, R. M. Vernon, Z. Siddiqui, M. Krzeminski, R. Muhandiram, C. Zhao, N. Sonenberg, L. E. Kay and J. D. Forman-Kay, *Nature*, 2015, **519**, 106.
9 H. Lodish, A. Berk, S. L. Zipursky, P. Matsudaira, D. Baltimore and J. Darnell, *Molecular Cell Biology*, WH Freeman, 4th edn2000.
10 H. R. Hulett, *Nature*, 1970, **225**, 1248.
11 (*a*) A. Sorrenti, J. Leira-Iglesias, A. Sato and T. M. Hermans, *Nat. Commun.*, 2017, **8**, 15899; (*b*) M. A. Cardona and L. J. Prins, *Chem. Sci.*, 2020, **11**, 1518; (*c*) S. Maiti, I. Fortunati, C. Ferrante, P. Scrimin and L. J. Prins, *Nat. Chem.*, 2016, **8**, 725; (*d*) C. Pezzato and L. J. Prins, *Nat. Commun.*, 2015, **6**, 7790; (*e*) D. Pei, B. Liu, S. Zhao, X. Shu, J. Nie and Y. Chang, *ACS Appl. Bio Mater.*, 2021, **4**(4), 3532–3538; (*f*) S. Dhiman, A. Jain and S. J. George, *Angew. Chem., Int. Ed.*, 2017, **56**, 1329; (*g*) L. Heinen and A. Walther, *Sci. Adv.*, 2019, **5**, eaaw0590; (*h*) P. Solís Muñana, G. Ragazzon, J. Dupont, C. Z.-J. Ren, L. J. Prins and J. L.-Y. Chen, *Angew. Chem., Int. Ed.*, 2018, **57**, 16469; (*i*) S. Dhiman, A. Jain and S. J. George, *Angew. Chem., Int. Ed.*, 2017, **56**, 1329.
12 (*a*) J. Leira-Iglesias, A. Sorrenti, A. Sato, P. A. Dunne and T. M. Hermans, *Chem. Commun.*, 2016, **52**, 9009; (*b*) K. Jalani, S. Dhiman, A. Jain and S. J. George, *Chem. Sci.*, 2017, **8**, 6030; (*c*) I. Maity, N. Wagner, R. Mukherjee, D. Dev, E. Peacock-Lopez, R. Cohen-Luria and G. Ashkenasy, *Nat. Commun.*, 2019, **10**, 4636; (*d*) S. M. Morrow, I. Colomer and S. P. Fletcher, *Nat. Commun.*, 2019, **10**, 1011; (*e*) Y. Altay, I. A. B. Pijpers, L. K. E. A. Abdelmohsen and J. C. M. van Hest, *ChemSystemsChem*, 2020, **2**, e1900049; (*f*) B. Fan, Y. Men, S. A. P. van Rossum, G. Li and R. Eelkema, *ChemSystemsChem*, 2020, **2**, e1900028; (*g*) W. A. Ogden and Z. Guan, *ChemSystemsChem*, 2020, **2**, e1900030; (*h*) S. Yang, G. Schaeffer, E. Mattia, O. Markovitch, K. Liu, A. S. Hussain, J. Ottelé, A. Sood and S. Otto, *Angew. Chem., Int. Ed.*, 2021, **60**, 11344.
13 (*a*) J. Boekhoven, A. M. Brizard, K. N. K. Kowlgi, G. J. M. Koper, R. Eelkema and J. H. van Esch, *Angew. Chem., Int. Ed.*, 2010, **49**, 4825; (*b*) J. Boekhoven, W. E. Hendriksen, G. J. M. Koper, R. Eelkema and J. H. van Esch, *Science*, 2015, **349**, 1075; (*c*) B. G. P. van Ravensteijn, W. E. Hendriksen, R. Eelkema, J. H. van Esch and W. K. Kegel, *J. Am. Chem. Soc.*, 2017, **139**, 9763.
14 (*a*) I. Colomer, S. M. Morrow and S. P. Fletcher, *Nat. Commun.*, 2018, **9**, 2239; (*b*) I. Colomer, A. Borissov and S. P. Fletcher, *Nat. Commun.*, 2020, **11**, 176.
15 A. Jain, S. Dhiman, A. Dhayani, P. K. Vemula and S. J. George, *Nat. Commun.*, 2019, **10**, 450.
16 (*a*) S. Debnath, S. Roy and R. V. Ulijn, *J. Am. Chem. Soc.*, 2013, **135**, 16789; (*b*) C. G. Pappas, I. R. Sasselli and R. V. Ulijn, *Angew. Chem., Int. Ed.*, 2015, **54**, 8119.
17 (*a*) N. Singh, B. Lainer, G. J. M. Formon, S. De Piccoli and T. M. Hermans, *J. Am. Chem. Soc.*, 2020, **142**, 4083; (*b*) M. P. van der Helm, C.-L. Wang, B. Fan, M. Macchione, E. Mendes and R. Eelkema, *Angew. Chem., Int. Ed.*, 2020, **59**, 20604; (*c*) C. S. Wood, C. Browne, D. M. Wood and J. R. Nitschke, *ACS Cent. Sci.*, 2015, **1**, 504.
18 (*a*) A. Williams and I. T. Ibrahim, *Chem. Rev.*, 1981, **81**, 589; (*b*) M. A. Gilles, A. Q. Hudson and C. L. Borders, *Anal. Biochem.*, 1990, **184**, 244.
19 M. Tena-Solsona, B. Rieß, R. K. Grötsch, F. C. Löhrer, C. Wanzke, B. Käsdorf, A. R. Bausch, P. Müller-Buschbaum, O. Lieleg and J. Boekhoven, *Nat. Commun.*, 2017, **8**, 15895.
20 A. J. Lomant and G. Fairbanks, *J. Mol. Biol.*, 1976, **104**, 243.
21 H. J. Goren and M. Fridkin, *Eur. J. Biochem.*, 1974, **41**, 263.
22 (*a*) S. Bal, C. Ghosh, T. Ghosh, R. K. Vijayaraghavan and D. Das, *Angew. Chem., Int. Ed.*, 2020, **59**, 13506; (*b*) S. Bal, K. Das, S. Ahmed and D. Das, *Angew. Chem., Int. Ed.*, 2019, **58**, 244.
23 M. Tena-Solsona, J. Janssen, C. Wanzke, F. Schnitter, H. Park, B. Rieß, J. M. Gibbs, C. A. Weber and J. Boekhoven, *ChemSystemsChem*, 2021, **3**, e2000034.
24 (*a*) M. Tena-Solsona, C. Wanzke, B. Riess, A. R. Bausch and J. Boekhoven, *Nat. Commun.*, 2018, **9**, 2044; (*b*) I. M. Jayalath, H. Wang, G. Mantel, L. S. Kariyawasam and C. S. Hartley, *Org. Lett.*, 2020, **22**, 7567.

 This journal is © The Royal Society of Chemistry 2022

Published on 23 December 2021. Downloaded by Technical University of Munich on 2/3/2022 3:20:27 PM.

25 S. Borsley, D. A. Leigh and B. M. W. Roberts, *J. Am. Chem. Soc.*, 2021, **143**(11), 4414–4420.
26 N. Nakajima and Y. Ikada, *Bioconjugate Chem.*, 1995, **6**, 123.
27 D. H. Rich and J. Singh, in *Major Methods of Peptide Bond Formation*, ed. E. Gross and J. Meienhofer, Academic Press, 1979, vol. 1, p. 241.
28 C. Wanzke, M. Tena-Solsona, B. Rieß, L. Tebcharani and J. Boekhoven, *Mater. Horiz.*, 2020, **7**, 1397.
29 L. S. Kariyawasam and C. S. Hartley, *J. Am. Chem. Soc.*, 2017, **139**, 11949.
30 J. S. Moore and S. I. Stupp, *Macromolecules*, 1990, **23**, 65.
31 B. A. K. Kriebisch, A. Jussupow, A. M. Bergmann, F. Kohler, H. Dietz, V. R. I. Kaila and J. Boekhoven, *J. Am. Chem. Soc.*, 2019, **142**, 20837.
32 F. Schnitter and J. Boekhoven, *ChemSystemsChem*, 2021, **3**, e2000037.
33 L. S. Kariyawasam, J. C. Kron, R. Jiang, A. J. Sommer and C. S. Hartley, *J. Org. Chem.*, 2020, **85**, 682.
34 F. Schnitter, A. M. Bergmann, B. Winkeljann, J. Rodon Fores, O. Lieleg and J. Boekhoven, *Nat. Protoc.*, 2021, **16**, 3901.
35 C. M. Dobson, *Nature*, 2003, **426**, 884.
36 L. Szilák, J. Moitra and C. Vinson, *Protein Sci.*, 1997, **6**, 1273.
37 W. Zeng, C. Fan, X. Xing, H. Cheng, H. Fu, B. Ma, Z. Yang, R. Zhang and W. Zhang, *Giant*, 2021, 100067.
38 J. Heckel, S. Loescher, R. T. Mathers and A. Walther, *Angew. Chem.*, 2020, **60**, 7117.
39 M. M. Hossain, J. L. Atkinson and C. S. Hartley, *Angew. Chem., Int. Ed.*, 2020, **59**, 13807.
40 M. Stasi, A. M. i Sureda, L. Babl, S. Wunnava, C. Dirscherl, D. Braun, P. Schwille, H. Dietz and J. Boekhoven, *ChemRxiv*, 2021, DOI: 10.33774/chemrxiv-2021-w299m.
41 D. Zwicker, A. A. Hyman and F. Jülicher, *Phys. Rev. E: Stat., Nonlinear, Soft Matter Phys.*, 2015, **92**, 012317.
42 D. Zwicker, R. Seyboldt, C. A. Weber, A. A. Hyman and F. Jülicher, *Nat. Phys.*, 2017, **13**, 408.
43 P.-A. Monnard and P. Walde, *Life*, 2015, **5**, 1239.
44 N. Martin and J.-P. Douliez, *ChemSystemsChem*, 2021, **3**(6), e2100024.
45 (*a*) P. A. Bachmann, P. L. Luisi and J. Lang, *Nature*, 1992, **357**, 57; (*b*) P. L. Luisi and F. J. Varela, *Origins Life Evol. Biospheres*, 1989, **19**, 633.
46 (*a*) A. I. Oparin, *The origin of life*, 1953; (*b*) K. K. Nakashima, M. A. Vibhute and E. Spruijt, *Front. Mol. Biosci.*, 2019, **6**, DOI: 10.3389/fmolb.2019.00021.
47 B. C. Buddingh and J. C. M. van Hest, *Acc. Chem. Res.*, 2017, **50**, 769.
48 P. W. Voorhees, *Annu. Rev. Mater. Sci.*, 1992, **22**, 197.
49 C. Donau, F. Späth, M. Sosson, B. A. K. Kriebisch, F. Schnitter, M. Tena-Solsona, H.-S. Kang, E. Salibi, M. Sattler, H. Mutschler and J. Boekhoven, *Nat. Commun.*, 2020, **11**, 5167.
50 F. Späth, C. Donau, A. M. Bergmann, M. Kränzlein, C. V. Synatschke, B. Rieger and J. Boekhoven, *J. Am. Chem. Soc.*, 2021, **143**, 4782.
51 C. Wanzke, A. Jussupow, F. Kohler, H. Dietz, V. R. I. Kaila and J. Boekhoven, *ChemSystemsChem*, 2020, **2**, e1900044.
52 G. La Sorella, G. Strukul and A. Scarso, *Green Chem.*, 2015, **17**, 644.
53 (*a*) X. Lang, U. Thumu, L. Yuan, C. Zheng, H. Zhang, L. He, H. Zhao and C. Zhao, *Chem. Commun.*, 2021, **57**, 5786; (*b*) M. A. Würbser, P. S. Schwarz, J. Heckel, A. M. Bergmann, A. Walther and J. Boekhoven, *ChemSystemsChem*, 2021, **3**, e2100015.
54 D. A. Fletcher and R. D. Mullins, *Nature*, 2010, **463**, 485.
55 (*a*) T. Mitchison and M. Kirschner, *Nature*, 1984, **312**, 237; (*b*) E. D. Korn, M.-F. Carlier and D. Pantaloni, *Science*, 1987, **238**, 638.
56 K. Dai, J. R. Fores, C. Wanzke, B. Winkeljann, A. M. Bergmann, O. Lieleg and J. Boekhoven, *J. Am. Chem. Soc.*, 2020, **142**, 14142.
57 S. Mondal and D. Haldar, *New J. Chem.*, 2021, **45**, 4773.
58 B. Zhang, I. M. Jayalath, J. Ke, J. L. Sparks, C. S. Hartley and D. Konkolewicz, *Chem. Commun.*, 2019, **55**, 2086.
59 S. Bai, X. Niu, H. Wang, L. Wei, L. Liu, X. Liu, R. Eelkema, X. Guo, J. H. van Esch and Y. Wang, *Chem. Eng. J.*, 2021, **414**, 128877.
60 O. J. Dodo, L. Petit, C. W. H. Rajawasam, C. S. Hartley and D. Konkolewicz, *Macromolecules*, 2021, **54**(21), 9860–9867.
61 M. Cheng, C. Qian, Y. Ding, Y. Chen, T. Xiao, X. Lu, J. Jiang and L. Wang, ACS, *Mater. Lett.*, 2020, **2**, 425.
62 A. J. Bissette and S. P. Fletcher, *Origins Life Evol. Biospheres*, 2015, **45**, 21.
63 (*a*) P. A. Bachmann, P. Walde, P. L. Luisi and J. Lang, *J. Am. Chem. Soc.*, 1990, **112**, 8200; (*b*) P. A. Bachmann, P. L. Luisi and J. Lang, *Chimia*, 1991, **45**, 266; (*c*) P. A. Bachmann, P. Walde, P. L. Luisi and J. Lang, *J. Am. Chem. Soc.*, 1991, **113**, 8204.
64 B. Rieß, C. Wanzke, M. Tena-Solsona, R. K. Grötsch, C. Maity and J. Boekhoven, *Soft Matter*, 2018, **14**, 4852.
65 P. S. Schwarz, S. Laha, J. Janssen, T. Huss, J. Boekhoven and C. A. Weber, *Chem. Sci.*, 2021, **12**, 7554.
66 L. Tebcharani, C. Wanzke, T. M. Lutz, J. Rodon-Fores, O. Lieleg and J. Boekhoven, *J. Controlled Release*, 2021, **339**, 498.
67 P. S. Schwarz, L. Tebcharani, J. E. Heger, P. Müller-Buschbaum and J. Boekhoven, *Chem. Sci.*, 2021, **12**, 9969.
68 M. Schliwa and G. Woehlke, *Nature*, 2003, **422**, 759.
69 (*a*) R. D. Astumian, *Chem. Sci.*, 2017, **8**, 840; (*b*) C. Pezzato, C. Cheng, J. F. Stoddart and R. D. Astumian, *Chem. Soc. Rev.*, 2017, **46**, 5491.
70 (*a*) J. D. Badjić, V. Balzani, A. Credi, S. Silvi and J. F. Stoddart, *Science*, 2004, **303**, 1845; (*b*) J. D. Badjic, C. M. Ronconi, J. F. Stoddart, V. Balzani, S. Silvi and A. Credi, *J. Am. Chem. Soc.*, 2006, **128**, 1489; (*c*) J. Wu, K. C.-F. Leung, D. Benítez, J.-Y. Han, S. J. Cantrill, L. Fang and J. F. Stoddart, *Angew. Chem., Int. Ed.*, 2008, **47**, 7470.
71 (*a*) S. A. Vignon, T. Jarrosson, T. Iijima, H.-R. Tseng, J. K. M. Sanders and J. F. Stoddart, *J. Am. Chem. Soc.*, 2004, **126**, 9884; (*b*) D. S. Marlin, D. González Cabrera, D. A. Leigh and A. M. Z. Slawin, *Angew. Chem., Int. Ed.*, 2006, **45**, 77; (*c*) D. S. Marlin, D. González Cabrera, D. A. Leigh and A. M. Z. Slawin, *Angew. Chem., Int. Ed.*, 2006, **45**, 1385.
72 M. R. Wilson, J. Solà, A. Carlone, S. M. Goldup, N. Lebrasseur and D. A. Leigh, *Nature*, 2016, **534**, 235.